JOURNAL OF SOLID STATE CHEMISTRY **121,** 167–173 (1996)
ARTICLE NO. 0024

Ordered and Defect Structures in the UO_2–WO_3 System, Revealed by HREM

Margareta Sundberg and Bengt-Olov Marinder

Department of Inorganic Chemistry, Arrhenius Laboratory, Stockholm University, S-106 91 Stockholm, Sweden

Received May 23, 1995; accepted September 13, 1995

The four phases $U(WO_4)_2$, UW_3O_{11}, UW_4O_{14}, and UW_5O_{17} in the UO_2–WO_3 system have been identified by X-ray powder diffraction and high-resolution electron microscopy. $U(WO_4)_2$ is isotypic with the orthorhombic modification of $Th(MoO_4)_2$, with eight-coordinated uranium and four-coordinated tungsten. The other three are related to orthorhombic UMo_2O_8. The structure of UW_3O_{11} is new and has been deduced from HREM images and verified by simulated image calculations. The unit cell dimensions are $a = 13.802(2)$, $b = 7.3998(4)$, and $c = 4.0707(4)$ Å. All three structures are built up of corner-sharing WO_6 octahedra in ReO_3-type slabs of different width (n). The WO_3 slabs are intergrown with slabs of edge-sharing polyhedra of pentagonal UO_7 bipyramids (PB). These phases are denoted (n)-PB. Some isolated defects in terms of varying widths of the WO_3 slabs have been observed. An ordered intergrowth structure, denoted $(4,3,3,3)_2$-PB, of (3)-PB and (4)-PB elements has also been found.

INTRODUCTION

Several phases in the system UO_2–MoO_2–MoO_3–WO_3 have been prepared and studied by high-resolution electron microscopy (HREM) combined with X-ray powder and single-crystal diffraction (1–3). The phases observed were either oxides containing uranium and molybdenum or uranium, molybdenum, and tungsten. In no case was an oxide containing solely uranium and tungsten found. Samples with bulk compositions $UMoW_{13}O_{44}$ and $UMo_{10}O_{31}$ have previously been examined by HREM.

Results from a phase analysis study, based on X-ray powder diffraction technique, have been reported from part of the UO_2–MoO_2–MoO_3 system (4). HREM and X-ray powder diffraction were recently used in an investigation of the subsystem UO_2–MoO_3 (5).

Some of the observed phases in the UO_2–MoO_2–MoO_3–WO_3 system can be described as intergrowth of slabs of ReO_3 type with tilted octahedra, and slabs of hexagonal tungsten bronze (HTB) type. In the latter, the hexagonal tunnels are occupied by chains of –O–U–O–U– atoms, thereby forming coordination polyhedra of hexagonal UO_8 bipyramids (HB). Quite often, however, some of the U positions are vacant, resulting in the formation of UO_2 entities in the tunnels. Other phases in the system consist of slabs of ReO_3 type intergrown with slabs of edge-sharing polyhedra of pentagonal UO_7 bipyramids (PB).

The slabs encountered in structures of these types, i.e., the ReO_3 type, the HB type, and the PB type, are infinite in two dimensions. In an ReO_3-type slab the width is determined by the number (n) of octahedra across the slab. Similarly, any number of hexagonal tunnel rows may form an HB-type slab, while only a single row of pentagonal bipyramids constitutes a PB-type slab. It is obvious that the slab types described make possible the great variety of crystal structures actually observed, including also disordered structures and defects of various kinds.

In the present investigation we have limited ourselves to the system UO_2–WO_3, i.e., with no molybdenum oxides present. Rather few data about the phase conditions in this system seem to be available. An orthorhombic X-ray diffraction pattern of $U(WO_4)_2$ similar to that of $Th(WO_4)_2$ has been reported (6, 7). Another orthorhombic phase, $U_5W_{19}O_{67}$, assumed to be structurally related to U_3O_8, has also been observed (8).

EXPERIMENTAL

Samples of various compositions $UO_2 : m\ WO_3$ ($1 \leq m \leq 6$) were synthesized by heating appropriate mixtures of U_3O_8, WO_3, and tungsten metal powder in evacuated silica tubes at 970 K for 1 day and at 1070 or 1170 K for 3 or 4 days. At the end of the heating period the samples were cooled by removing the tubes from the furnace. U_3O_8 was prepared by heating $UO_2(NO_3)_2 \cdot 6H_2O$ at 1020 K. WO_3 (99.9%) was delivered by Koch-Light laboratories Ltd., England and tungsten metal powder by Kebo AB, Stockholm.

X-ray patterns were registered in a Guinier–Hägg focusing camera with monochromatized Cu$K\alpha_1$ radiation. Si or KCl was used as an internal theta-standard. The electron microscopy specimens were prepared in the following way. A small amount of the sample was crushed in an agate

0022-4596/96 $12.00

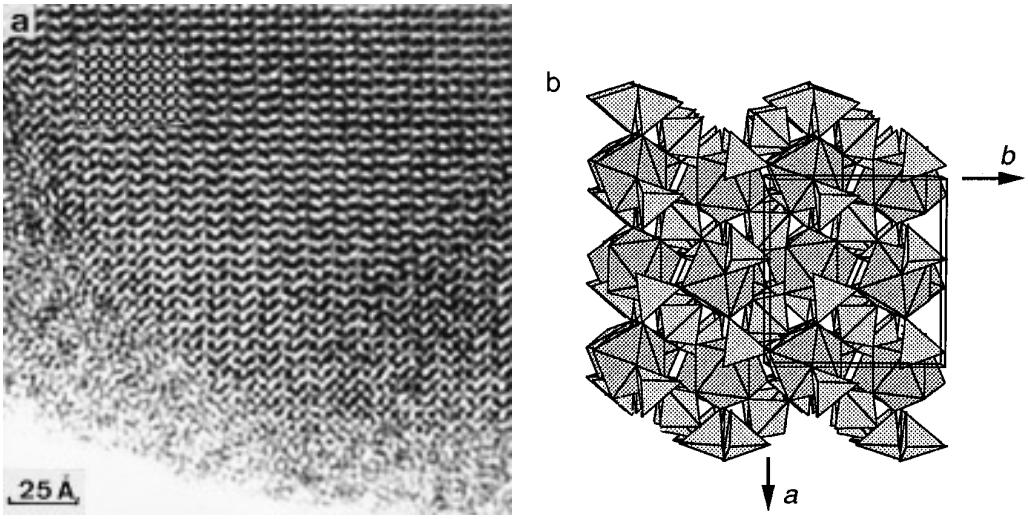

FIG. 1. (a) HREM image of $U(WO_4)_2$ projected along [001]. A simulated image is inserted, calculated for a crystal thickness ≈30 Å and a defocus value −200 Å. (b) Structure model of $U(WO_4)_2$. Uranium is coordinated to eight oxygen atoms in the form of a slightly distorted square antiprism (dark-shaded). Tungsten is tetrahedrally coordinated by oxygen atoms. The tetrahedra are light-shaded. This drawing is produced with ATOMS by Shape Software.

mortar and dispersed in *n*-butanol. Drops of the resultant suspension were put onto a perforated carbon film supported by a Cu grid. HREM studies were performed in a JEOL JEM 200CX transmission electron microscope, which was equipped with a top-entry, double-tilt goniometer stage with tilt angles of ±10°. The microscope was operated at 200 kV. The radius of the objective aperture used corresponds to approximately 0.41 $Å^{-1}$ in reciprocal space. Simulated HREM images were calculated by utilization of a locally modified version of the SHRLI suite of programs (9). A JEOL 2000FX-II transmission electron microscope fitted with a LINK QX200 X-ray analysis system was used for electron diffraction studies of thin crystal fragments in combination with the EDS analysis.

RESULTS

Both X-ray powder diffraction and electron microscopy studies showed that multiphase specimens had been formed. In some of the samples small amounts of UO_2 and WO_3 were found. Moreover, a cubic U_xWO_3 phase was observed in most of the specimens.

$U(WO_4)_2$ Structure

An image of one of the phases found in the bulk samples with $m = 1$ and 2 is illustrated in Fig. 1. The electron diffraction study showed a lattice with the parameters $a \approx 10.2$, $b \approx 9.6$, and $c \approx 14.3$ Å. EDS analyses of the fragments indicated an U : W ratio of about 1 : 2. The Guinier powder pattern of the sample with $m = 2$ could be indexed with a unit cell of orthorhombic symmetry with $a = 10.228(3)$, $b = 9.572(1)$, and $c = 14.296(3)$ Å. These values are close to those previously given for the $U(WO_4)_2$ compound (6): $a = 10.245 \pm 0.005$, $b = 9.545 \pm 0.003$, and $c = 14.26 \pm 0.01$ Å. $U(WO_4)_2$ has been reported as isostructural with $Th(WO_4)_2$ (6) and the orthorhombic modification of $Th(MoO_4)_2$ (10).

The HREM image in Fig. 1a was taken of a thin crystal fragment. During HREM observation the structure slowly decomposed to an amorphous phase, as can be seen at the edge of the fragment. The unit cell dimensions show that there is no obvious projection suitable for HREM studies of $U(WO_4)_2$, as there is no short repeat distance in the structure. As $U(WO_4)_2$ has been reported to be isostructural with $Th(MoO_4)_2$, the fractional coordinates given in a single crystal X-ray study of the latter compound (11) were used as positional parameters in our simulated image calculations of the $U(WO_4)_2$ structure. Sets of theoretical images were calculated for different crystal thicknesses and defocus values. There is good agreement between the observed HREM image and the calculated image in the insert in Fig. 1a, which verifies the model. All fragments examined were well ordered. No defects or intergrowth structures were observed.

The crystal structure of $U(WO_4)_2$ is shown in Fig. 1b. The uranium atoms are eight-coordinated in the form of slightly distorted square antiprisms. Tungsten atoms are four-coordinated in nearly regular WO_4 tetrahedra. The two types of coordination polyhedra are mutually connected by sharing of oxygen corner atoms.

Both U_xWO_3 and UO_2 fragments have been found by electron diffraction in combination with EDS analysis in

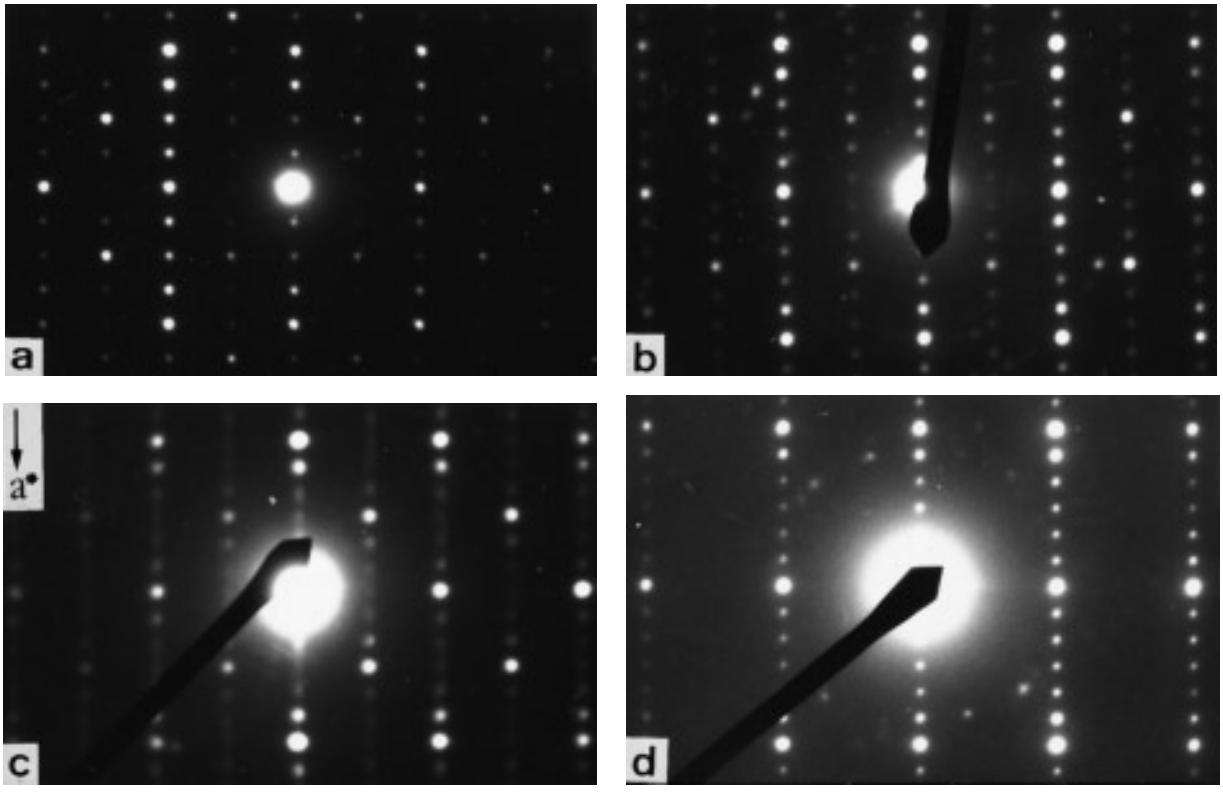

FIG. 2. Electron diffraction patterns in [001] projection (a) UW_3O_{11} ((3)-PB) (b) UW_4O_{14} ((4)-PB). Electron diffraction patterns of UW_5O_{17} crystals viewed along (c) [001] and (d) [010].

the samples with $m = 1$ and 2. Rozanova *et al.* (6) have previously reported that $U(WO_4)_2$ decomposed slowly with formation of the phases U_xWO_3 and $(U, W)O_{2+x}$ at an annealing temperature of 1273 K. It should be mentioned that our electron microscopy study also indicated the formation of a phase with the U : W ratio approximately equal to 1 : 1. This structure will be discussed elsewhere.

Ordered (n)-PB Structures

Electron microscopy studies of thin crystal fragments from the bulk specimens with $3 \leq m \leq 6$ showed that three related phases of (n)-PB-type structure were present. The most frequently observed phases (3)-PB and (4)-PB seemed to be well ordered, as the reflection spots in the electron diffraction patterns were sharp (Figs. 2a and 2b). Streaking of the reflections along the a^* axis was often observed in the electron diffraction patterns taken from (5)-PB-type fragments (Fig. 2c). The streaking indicates the presence of ReO_3-type slabs of varying widths, but $n = 5$ is the dominating slab thickness in the examined fragment. No ordered fragments of (n)-PB structure with $n \geq 6$ have been observed. From the electron diffraction study it was also obvious that no fragment of (n)-HB-type structure could be found in the investigated samples.

All three (n)-PB phases have orthorhombic unit cells with two axes of almost the same dimensions; they differ only in the length of the third axis. The following unit cell dimensions were obtained from Guinier data:

$a = 13.802(2)$, $b = 7.3998(4)$, and $c = 4.0707(4)$ Å ((3)-PB phase);

$a = 35.048(3)$, $b = 7.3962(6)$, and $c = 4.0514(4)$ Å ((4)-PB phase).

The latter structure is *C* centered. The electron diffraction patterns in Figs. 2c and 2d are taken from thin crystal fragments of the (5)-PB structure. The lattice parameters were calculated to be: $a = 21.3$, $b = 7.4$, and $c = 4.05$ Å. There is no indication of a doubling of the a axis.

The HREM image in Fig. 3a shows a well-ordered fragment of the (3)-PB phase. It is recorded at a defocus value where the metal atoms are imaged with white contrast. The contrast features in Fig. 3a are interpreted as slabs of corner-sharing WO_6 octahedra of ReO_3 type, with a width of three octahedra. Figure 3a also shows that almost straight lines of white dots (four of which are marked by arrows) connect the slabs. However, the interpretation of these contrast features is not straightforward. From the electron diffraction pattern in Fig. 2a and the unit cell dimensions, however, it was apparent that the white dots connecting the WO_3 slabs correspond to projected –O–U–

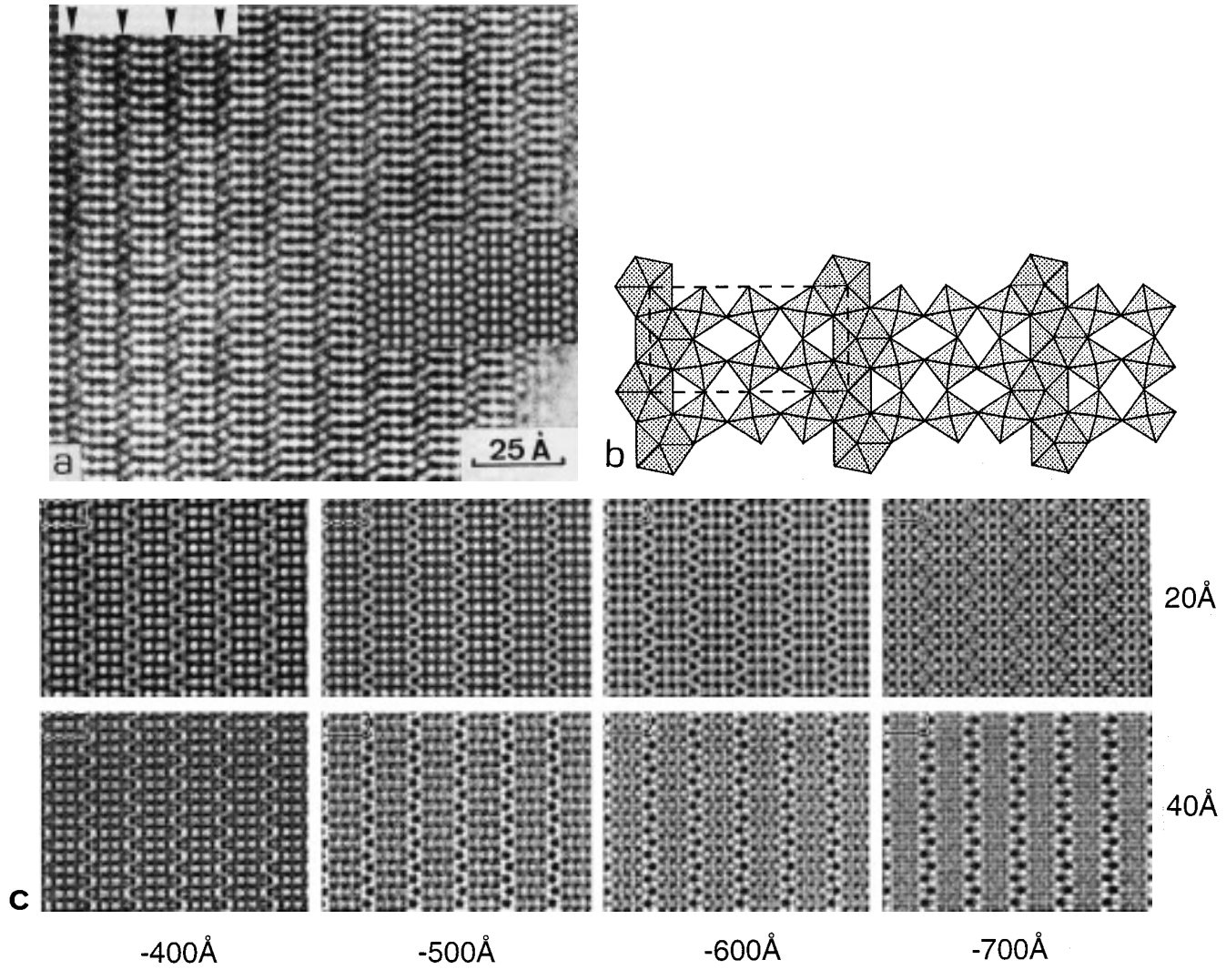

FIG. 3. (a) HREM image of a UW_3O_{11} crystal in [001] projection. The metal atoms appear white. A simulated image is shown in the insert: thickness ≈20 Å, defocus value −900 Å. (b) Corresponding structure model. (c) Simulated images of the structure model in b.

O–U– chains, arranged as in the (*n*)-PB-type structures. The structure model is shown in Fig. 3b. The framework composition is UW_3O_{11}, which was later confirmed by EDS analysis. Theoretical images were calculated, using the parameters derived from the HREM image and given in Table 1. There is good agreement between the experimental image and the calculated image in the insert in Fig. 3a. The set of calculated images in Fig. 3c shows that there is a narrow region around a defocus value of −500 Å and a crystal thickness of ≈20 Å where a direct correspondence between the black contrast in the recorded HREM image and the metal atom arrangement in the structure is obtained. Previous image simulations of the UMo_2O_8 and the UMo_5O_{16} structures have shown (1) that it is difficult to distinguish between the two structures, (2)-PB and (2)-HB, from only HREM images recorded at Scherzer focus

TABLE 1
Atomic Coordinates for the UW_3O_{11} Structure

Atom	Site	*x*	*y*	*z*
U1	2(*a*)	0.96	0	0
W1	2(*d*)	1/2	1/4	0.0
W2	4(*e*)	0.25	0.25	0.0
O1	2(*b*)	0.96	0	1/2
O2	2(*d*)	1/2	1/4	0.5
O3	4(*e*)	0.25	0.25	0.5
O4	2(*a*)	0.27	0	0
O5	2(*a*)	0.45	0	0
O6	2(*a*)	0.82	0	0
O7	4(*e*)	0.09	0.17	0.0
O8	4(*e*)	0.36	0.33	0.0

Note. Spacegroup $P22_12$(No. 17) with the general positions $x, y, z; x, \bar{y}, \bar{z}; \bar{x}, 1/2 + y, \bar{z}; \bar{x}, 1/2\text{-}y, z$.

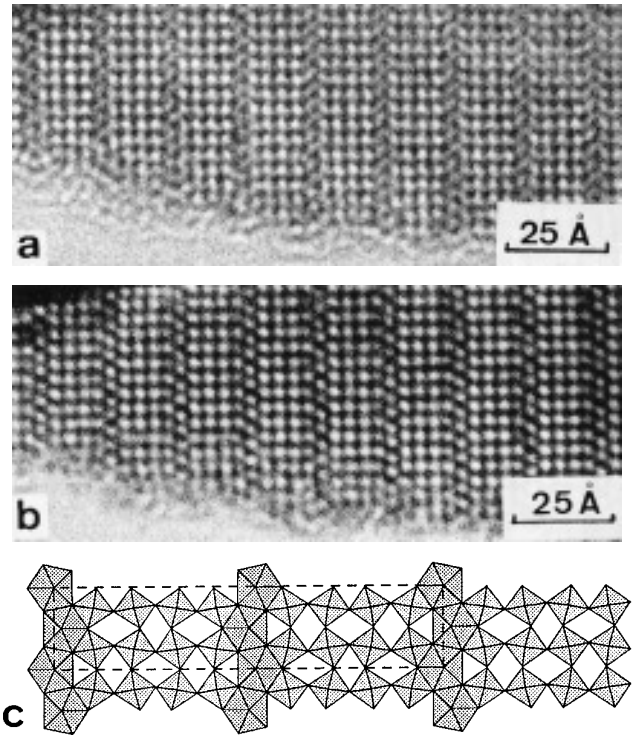

FIG. 4. HREM images showing an ordered fragment of UW_4O_{14} at two defocus values, (a) −500 Å and (b) −900 Å. The projected metal atoms appear as black dots in (a) and white dots in (b). An idealized structure model projected along [001] is illustrated in (c).

(−500 Å). The UW_3O_{11} phase discussed here has not previously been observed.

HREM images taken of an ordered (4)-PB-type structure at two defocus values are shown in Figs. 4a and 4b and a structure model in Fig. 4c. The width of the distorted ReO_3 slabs corresponds to four WO_6 octahedra. These can also be seen in Fig. 4a as four black spots. The stoichiometry of the unit cell is UW_4O_{14}. The metal atom content was confirmed by EDS analysis.

Defects and Intergrowth Structures

Defects were not common in the UW_3O_{11} and UW_4O_{14} structures. The low-magnification micrograph in Fig. 5 illustrates an example of isolated defects observed in a (3)-PB-type fragment. Single slabs, two and four octahedra wide, can be seen here. It should be mentioned that larger areas consisting of ordered WO_3 slabs with a width of two octahedra have not been observed so far. This might indicate that a UW_2O_8 structure isotypic with orthorhombic UMo_2O_8 (12) is not favored. In this connection it is interesting to note that there exists an extended solid solution $U(Mo_{1-x}W_x)_2O_8$(orth). A solid solution with up to $x = 0.7$, annealed at 1270 K and then slowly cooled, shows lattice parameters based on the UMo_2O_8(orth.) structure (13).

An ordered intergrowth of (3)- and (4)-PB slabs is shown in Fig. 6. Here, isolated (4)-PB slabs occur, regularly separated by three (3)-PB slabs. The electron diffraction pattern insert confirms this, showing a clear splitting of reflections. A structure model is shown in Fig. 6b. The unit cell dimensions are $a \approx 118$, $b \approx 7.4$, and $c \approx 4.1$ Å. The structure should be denoted $(4,3,3,3)_2$-PB (1,5,14). It can be considered as an ordered intergrowth structure of (3)-PB and (4)-PB elements.

CONCLUDING REMARKS

It has been shown above that the UW_2O_8 phase is isotypic with $Th(MoO_4)_2$ and not related to the (n)-PB-type structures UW_3O_{11}, UW_4O_{14}, and UW_5O_{17}. The formula should preferably be given as $U(WO_4)_2$ and the compound considered as an M^{+4} tungstate. The two structure types differ in coordination of both the uranium and of the tungsten atoms. In $U(WO_4)_2$ uranium is eight-coordinated and tungsten is four-coordinated, while in the (n)-PB structures uranium is seven-coordinated and tungsten is six-coordinated. It should be noted that tetrahedral coordination of W^{+6} is common both in the $M^{+2}WO_4$ and in the $M_2^{+3}(WO_4)_3$ tungstates (15).

In our studies of the UO_2–WO_3 system we have found one new compound of stoichiometry UW_3O_{11} and confirmed the formation of the related phases UW_4O_{14} and UW_5O_{17}. The latter two structures have previously been deduced from HREM images taken of crystals from a $UMoW_{13}O_{44}$ sample (2). No analyses of the Mo content in the crystals were made at that time. Our electron diffraction results from the UW_5O_{17} compound also showed that the longest axis is 21.3 Å, which is half the previously reported value (2).

The three structures UW_3O_{11}, UW_4O_{14}, and UW_5O_{17}

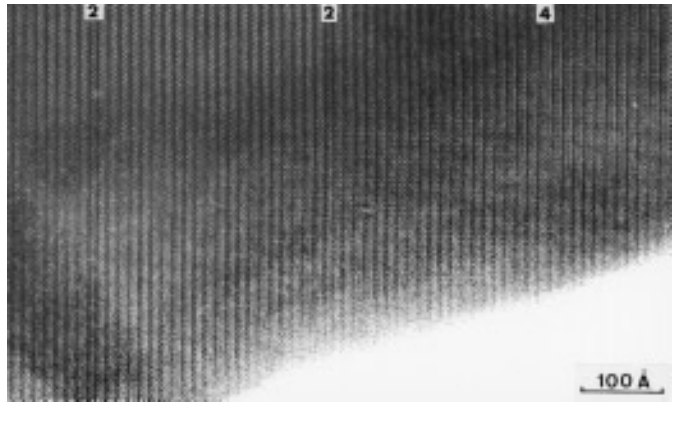

FIG. 5. A low-magnification micrograph of a UW_3O_{11} fragment showing a few isolated defects. Slabs of widths $n = 2$ and $n = 4$ are marked.

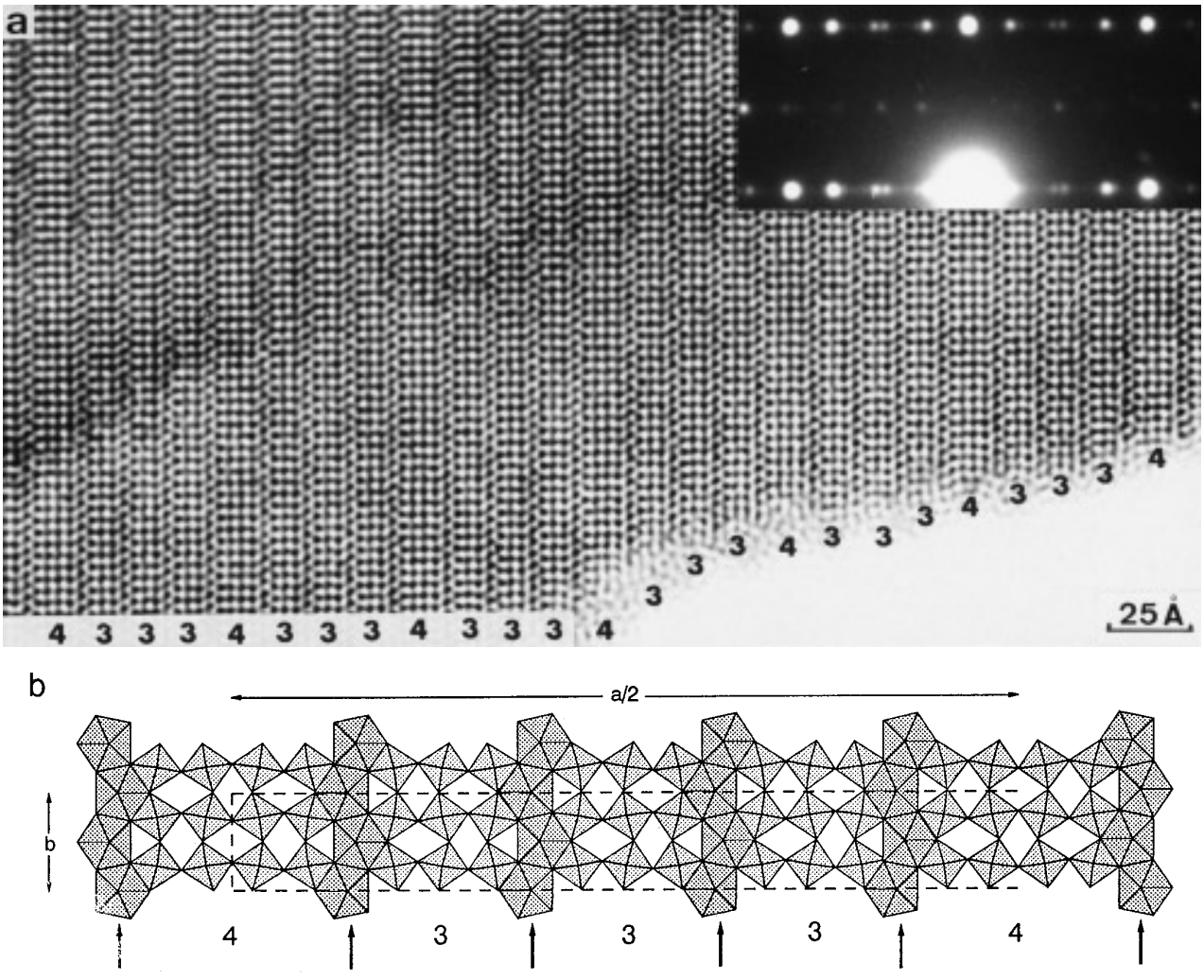

FIG. 6. (a) HREM image of a UW_3O_{11} fragment showing an ordered intergrowth structure $(4,3,3,3)_2$-PB. The subscript indicates that the sequence has to be taken twice to describe the arrangement along the *a* axis. The corresponding electron diffraction pattern in the insert shows splitting of reflections. (b) The idealized structure model $(4,3,3,3)_2$-PB, corresponding to the composition $U_4W_{13}O_{47}$.

are closely related and differ only in the width of the WO_3 slabs. They can be considered as the members $n = 3$, 4, and 5 of the homologous series of complex uranium oxides with the general formula $UO \cdot M_nO_{3n+1}$, where M = Mo, W and n corresponds to the number of octahedra across the ReO_3-type slab (1). As the structures contain pentagonal UO_7 bipyramids, the related phases are denoted (n)-PB. No ordered members with $n > 5$ have been found so far, nor have any HB phases been observed. Moreover, WO_3-type slabs of width $n = 2$ occurred only as single isolated defects in the UW_3O_{11} structure. Varying the annealing conditions of time and temperature and extending the composition range of $UO_2:WO_3$ to $m > 6$ might therefore be worthwhile. Such work is now in progress.

ACKNOWLEDGMENT

We are grateful to Jaroslava Östberg for technical assistance with the photographic work. This study has been supported by the Swedish Natural Science Research Council.

REFERENCES

1. M. Sundberg and V. Tabachenko, *Microsc. Microanal. Microstruct.* **1,** 373 (1990).
2. N. D. Zakharov, M. A. Gribeluk, B. K. Vainshtein, O. N. Rozanova, K. Uchida, and S. Horiuchi, *Acta Crystallogr. Sect. B* **39,** 575 (1983).
3. N. D. Zakharov, M. A. Gribelyuk, B. K. Vainshtein, L. M. Kovba, and S. Horiuchi, *Acta Crystallogr. Sect. A* **44,** 821 (1988).
4. O. G. D'Yachenko, V. V. Tabachenko, and L. M. Kovba, *Russ. J. Inorg. Chem.* **38,** 194 (1993).

5. M. Sundberg and B.-O. Marinder, *Eur. J. Solid State Inorg. Chem.* **31,** 855 (1994).
6. O. N. Rozanova, V. K. Trunov, and L. M. Kovba, *Inorg. Mater.* (*USSR*) **2,** 273 (1966).
7. B. Ampe, J. M. Leroy, D. Thomas, and G. Tridot, *Rev. Chim. Minér.* **5,** 789 (1968).
8. O. N. Rozanova, L. M. Kovba, and V. K. Trunov, *Sov. Radiochem.* **13,** 317 (1971).
9. M. O'Keefe, P. R. Buseck, and S. Iijima, *Nature* (*London*) **274,** 322 (1978).
10. W. Freundlich and M. Pagès, *C.R. Acad. Sc. Paris Sér. C* **269,** 392 (1969).
11. T. L. Cremers, P. G. Eller, and R. A. Penneman, *Acta Crystallogr. Sect. C* **39,** 1165 (1983).
12. T. L. Cremers, P. G. Eller, R. A. Penneman, and C. C. Herrick, *Acta Crystallogr. Sect. C* **39,** 1163 (1983).
13. O. N. Rozanova, L. M. Kovba, and V. K. Trunov, *Vestn. Mosk. Univ. Ser. 2 Khim.* **23,** 100 (1968).
14. A. Hussain and L. Kihlborg, *Acta Crystallogr. Sect. A* **32,** 551 (1976).
15. T. Ekström and R. J. D. Tilley, *Chem. Scr.* **16,** 1 (1980).